Screened test-charge - test-charge interaction in the two-dimensional electron gas: bound states

1997 J. Phys.: Condens. Matter 9 6885

(http://iopscience.iop.org/0953-8984/9/32/011)

J. Phys.: Condens. Matter **9** (1997) 6885–6900. Printed in the UK PII: S0953-8984(97)83210-9

Screened test-charge–test-charge interaction in the two-dimensional electron gas: bound states

A Gold† and A Ghazali‡

† Laboratoire de Physique des Solides§, Université Paul Sabatier, 118 Route de Narbonne, 31062 Toulouse, France

‡ Groupe de Physique des Solides§, Universités Paris 7&6, 2 place Jussieu, 75251 Paris, France

Received 7 April 1997

Abstract. We study the test-charge–test-charge interaction when screening effects of a two-dimensional electron gas are taken into account. The Schrödinger equation is solved in the momentum space by diagonalizing the corresponding matrix and the results are compared with variational calculations. For two *positive* (or *negative*) test-charges *bound states* are obtained for low electron densities when many-body effects are incorporated in the screening function. For a density larger than a critical density, $r_s < r_{sc} \approx 2.0$ (r_s is the Wigner–Seitz parameter), no bound states are found. Below the critical density, $r_s > r_{sc}$, the number of bound states and their energy increase with decreasing density and the ground-state binding energy saturates near -0.65 Rydberg*. Finite-width effects for quantum wells are also discussed. We present new results for bound states between a *positive* and a *negative* test charge and we discuss effects of exchange and correlation on the binding energies.

1. Introduction

It is known that a test charge in a three-dimensional electron gas is screened at large distances and the screened potential exhibits Friedel oscillations, which occur already within the framework of the random-phase approximation (RPA) [1]. The motivation for this paper is to understand the possibility of a Coulomb interaction-induced attraction in the electron gas between two equally charged particles. Such a possibility was suggested in the literature in the early 1960s and studied for a short-range potential [2]. In the low-density region a Wigner crystal is expected [3]. In the present paper we consider test-charges with charge $q = \pm e$ (and no spin), which are distinguishable from the electrons responsible for the screening.

For the two-dimensional electron gas it was demonstrated [4] that many-body effects described by the local-field correction (LFC) strongly enhance Friedel oscillations: many-body effects in the low-density regime give rise to bound states between two equally charged test particles. The calculated binding energies for quasi-one-dimensional [5] and two-dimensional [6] electron gases are in the range of 1 Rydberg. These results have been obtained by a variational method [5] and by a multiple scattering approach [6]. Here we study the two-dimensional electron gas by solving the Schrödinger equation and by using a variational method. We use the concept of the LFC included in the dielectric screening function within the formulation of Singwi, Tosi, Land and Sjölander (STLS) [7–11].

§ The 'Laboratoire de Physique des Solides' and the 'Groupe de Physique des Solides' are 'Laboratoires associés au Centre National de la Recherche Scientifique (CNRS)'.

0953-8984/97/326885+16$19.50

We report in this paper large bound-state energies found for screened repulsive test charges when the LFC is taken into account. This means that in two dimensions many-body effects for the screening function are very important. For the ground state the electron density is strongly decreased around the charged centre in order to avoid the repulsive Coulomb potential at small distances. Let us assume that we place two negative (or positive) test charges into a metal and the screening being provided by the electrons of the metal. Bound states should exist for $r_s > r_{sc} = 2$ (r_s is the Wigner–Seitz parameter). The like-charge attraction could lead to bound pairs of charge $\pm 2e$ and to superconductivity.

In the ideally two-dimensional hydrogen-like atom [12] the binding energy is enhanced compared with the binding energy of the hydrogen atom in three dimensions. For, ideally, two-dimensional systems the width perpendicular to the plane is zero. Realistically two-dimensional systems (quantum wells) are characterized by a finite width perpendicular to the plane and the binding energy depends on this width [13]. Moreover, the screened potential within the RPA always has a bound state and screening effects are not strong enough to make the binding energy vanish [13–15]. We discuss the effects of many-body effects on the ground-state binding energy and we present new results for the bound-state energy of excited states and Mott's critical density for excited states. We believe that the results of the present paper are relevant for the physics of excitons in the metallic regime and for charged impurities in two-dimensional metals.

The paper is organized as follows. In section 2 we describe the model and the theory. Our results for screened repulsive test charges are given in section 3. In section 4 we present our results for screened attractive test charges. We discuss our results in section 5 and we conclude in section 6.

2. Model and theory

2.1. The screened Coulomb interaction

As the model we use a two-dimensional electron gas with a parabolic dispersion. Distances are expressed in units of the effective Bohr radius $a^* = \varepsilon_L/m^*e^2$ with the Planck constant $h = 2\pi$; m^* is the effective mass and ε_L is the dielectric constant of the background material. We suppose that one test charge is fixed in space, otherwise the reduced mass should be used. Energy values are expressed in units of the effective Rydberg (Rydberg$^* = m^*e^4/2\varepsilon_L^2$). The density parameter r_s is given by $r_s = 1/[\pi N_A^{*2}]^{1/2}$ and $r_s a^*$ is the Wigner–Seitz radius. $N = k_F^2/2\pi$ is the two-dimensional electron density and k_F is the Fermi wavenumber with $k_F a^* = 2^{1/2}/r_s$. The Fermi energy ε_F is given as $\varepsilon_F/\text{Rydberg}^* = 2/r_s^2$.

The Coulomb interaction potential in the Fourier space between a (fixed) negative (or positive) test charge and another negative (or positive) test charge is repulsive and given by $V_t(q) = 2\pi e^2/\varepsilon_L q$. If the interaction is screened by an electron gas the screened interaction potential $V_{sc,t}(q)$ is written as $V_{sc,t}(q) = V_t(q)/\varepsilon(q)$. The dielectric function $\varepsilon(q)$ is given by [1]

$$\frac{1}{\varepsilon(q)} = 1 - \frac{V(q)\boldsymbol{X}_0(q)}{1 + V(q)[1 - G(q)]\boldsymbol{X}_0(q)} \tag{1}$$

where $\boldsymbol{X}_0(q)$ is the Lindhard function in two dimensions [16] and $V(q)$ is the bare interaction potential $V(q) = 2\pi e^2/\varepsilon_L q$.

In our calculation we use for $G(q)$ the sum-rule approximation [10] of the STLS approach. However, instead of parametrizing the LFC by two coefficients we use three

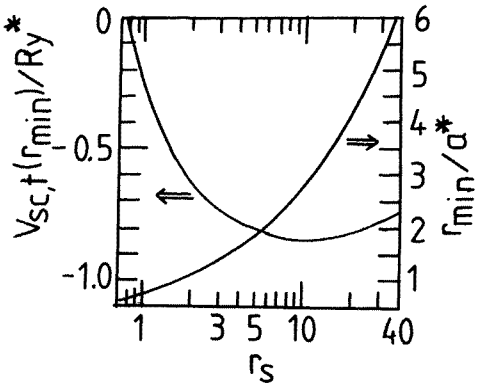

Figure 1. $V_{sc,t}(r_{\min})$ and $r_{\min}$ versus r_s as calculated by using $G(q)$ in equation (2).

coefficients in order to satisfy the compressibility sum rule. The LFC is given by [11]

$$G(q) = r_s^{2/3} \frac{1.402q}{[2.644q_0^2 C_1(r_s)^2 + q^2 C_2(r_s)^2 - q_0 q C_3(r_s)]^{1/2}} \tag{2}$$

where $q_0 = 2^{1/2}/r_s^{2/3}a^*$ is a characteristic wavenumber. The coefficient $C_1(r_s)$ is determined by the compressibility sum rule [1] using the analytical expression for the compressibility available in the literature [17]. $C_2(r_s)$ is fixed by the Shaw–Kimball relation [18] $G(q \to \infty) = 1 - g(0)$ and the sum-rule approach: $C_2(r_s) = 1.402 r_s^{2/3}/[1-g(0)]$ [10]. For $g(0)$ we use the analytical expression [19] $g(0) = 1/2 I_0(2^{3/4} r_s^{1/2})^2$. $I_0(z)$ is the zero-order modified Bessel function. $C_3(r_s)$ is calculated using the relation between the pair-correlation function $g(0)$ and the static structure factor $S(q)$. It can be shown [11] that the LFC $G(q)$ reproduces Monte Carlo calculations for the static susceptibility [20].

The screened Coulomb interaction in real space is given by

$$V_{sc,t}(r) = \int_0^\infty \mathrm{d}q\, q\, J_0(qr) V_{sc,t}(q)/2\pi \tag{3}$$

where $J_0(x)$ is the zero-order Bessel function of the first kind. Representative examples for $V_{sc,t}(r)$ have been shown in [4]. A strong minimum was found in $V_{sc,t}(r)$ at $r = r_{\min}$. A systematic study of $r_{\min}$ and $V_{sc,t}(r_{\min})$ versus r_s, see figure 1, shows that $V_{sc,t}(r_{\min})$ presents a weak minimum of -0.85 Rydberg* at $r_s = 10$. $V_{sc,t}(r_m)$ becomes very small for $r_s < 1$. In the low-density range $r_{\min}$ is large compared to a^* and bound states are very extended in real space.

2.2. The Schrödinger equation

We solve the Schrödinger equation for a test charge moving in the external potential $V_{sc,t}(\boldsymbol{r})$. $V_{sc,t}(\boldsymbol{r})$ is a central potential and only depends on r. The angular dependence of the wavefunction $\psi(\boldsymbol{r})$ in the real space and in the momentum space is described by $\exp(\pm \mathrm{i} l\varphi)$. States with given quantum number $l > 0$ are degenerate ($g_l = 2$) and the $l = 0$ state is non-degenerate. States with different values of l are not degenerate: for the screened potential the accidental degeneracy of the bare Coulomb interaction is lifted.

Using $\psi(\boldsymbol{r}) = \phi_{n_r l}(r) \exp[\pm \mathrm{i} l\varphi]$ one obtains for $\phi_{n_r l}(r)$ a radial Schrödinger equation for the effective potential $V_{\mathrm{eff}}(r) = V_l(r) + V_{sc,t}(r)$ with $V_l(r) = l^2/2m^*r^2$. From general

arguments [12] it is clear that for $l > 0$ the behaviour of the wavefunction for small r is determined by $V_l(r)$ with $\phi_{n_r l}(r \to 0) \propto r^l$. In the momentum space the wavefunction is given by $\psi(\boldsymbol{q}) = \phi_{n_r l}(q)\exp(\pm \mathrm{i}l\varphi)$ with $\phi_{n_r l}(q \to 0) \propto q^l$. In the following we use as notation ϕ or ϕ_l for $\phi_{n_r l}$. The Schrödinger equation for the screened potential is solved numerically in the momentum space:

$$\frac{q^2}{2m}\psi(\boldsymbol{q}) + \frac{1}{4\pi^2}\int \mathrm{d}^2\,\boldsymbol{q}' V_{sc,t}(\boldsymbol{q}-\boldsymbol{q}')\psi(\boldsymbol{q}') = E\psi(\boldsymbol{q}). \tag{4}$$

Using polar coordinates, we have discretized the integral over $\boldsymbol{q}'$ in equation (4) according to a set of (q', φ'). The sampled values in q' and φ' are those used in Gauss routines for integration. Five adjacent intervals in q' and 12 in φ' are used to sample the integral. The Hamiltonian operator in equation (4) is discretized under the form of a matrix. The order of this matrix is 3000 [5×10 points for $0 \leqslant q'a^* < \infty$ and 12×5 points for $0 \leqslant \varphi' \leqslant 2\pi$]. The eigenenergy–eigenfunction problem is solved numerically by a standard method for matrix diagonalization.

Using a trial wavefunction $\phi_v(r)$ the variational energy E_{var} is given by

$$E_{\mathrm{var}} = \langle T\rangle + \langle V_l\rangle + \langle V_{sc,t}\rangle \tag{5}$$

where $\langle O\rangle$ means $\langle O\rangle = \int_0^\infty \mathrm{d}r r\phi_v(r) O \phi_v(r)$. In the following we denote the trial wavefunction by $\phi_{iv}(r)$ and the index i describes different forms. A Gaussian form is used for $i = 1, 2$ (sections 3 and 4.4) and an exponential form for $i = 3$–5 (section 4).

3. Screened repulsive test charges

3.1. Matrix diagonalization

For screened repulsive test charges and $r_s < 2.0$ no bound states are found. Between $2.0 < r_s < 3.9$ we found a single bound state. The bound state energy as a function of r_s is given in the inset of figure 2. The binding energy approaches zero at a critical density $r_{sc} = 2.0$. Our variational results are also shown in the inset and give a smaller binding energy with a critical density given by $r_{sc} = 2.4$. For $3.9 \leqslant r_s \leqslant 6.6$ we find three bound states, where the two last states ($l = 1$, $g_l = 2$) are degenerate.

The eigenfunctions $\psi(q, \varphi)$ which we obtain numerically are defined in the momentum space. In order to characterize the angular momentum l of the bound states we have studied (i) the behaviour of the wavefunction at small wavenumbers and (ii) the angular dependence of the wavefunction. The degeneracy only allows us to discriminate between $l = 0$ and $l \neq 0$. Using the angular symmetry of the wavefunction one can show that [12]

$$\phi_l(r) \propto \int_0^\infty \mathrm{d}q' q' J_l(q'r)\phi_l(q') \tag{6}$$

where $J_l(x)$ is the Bessel function of the first kind and order l. From equation (6) and $J_l(x) \propto x^l$ it follows immediately that $\phi_0(r \to 0) = \text{constant}$. Numerical results for the ground state $\psi(r, \varphi) = \phi_0(r)$ versus r are shown in figure 3 for $r_s = 10$. For $r = 0$ we find a very small finite value. This finite value decreases with increasing r_s. $\phi_0(r)$ shows a large peak at about $r^* = 2.8a^*$ which corresponds to the value $r_{\min}$ of the screened potential. The ground-state wavefunction in the q space is shown in figure 4. Note that near $qa^* = 0.64$ the wavefunction $\psi(q, \varphi) = \phi_0(q)$ changes its sign. For $r_s = 10$ our numerical results for the excited-state wavefunctions are shown in figure 5.

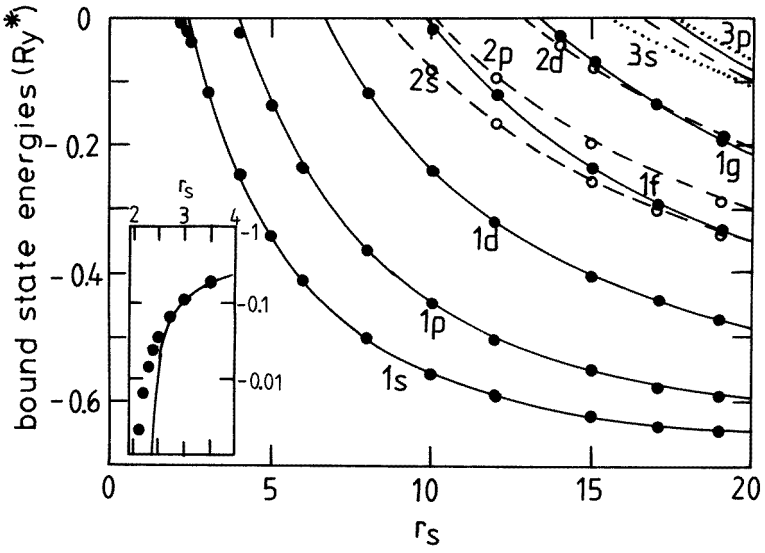

Figure 2. The bound-state energies $E_{\rm num}$ for screened repulsive test charges found by matrix diagonalization versus r_s. The full circles represent $n_r = 1$, the open circles represent $n_r = 2$ and the dotted curves represent $n_r = 3$. The variational results $E_{\rm min}$ are shown as full curves for $n_r = 1$ and as broken curves for $n_r = 2$. In the inset we show the ground-state energy versus r_s for $2 < r_s < 4$.

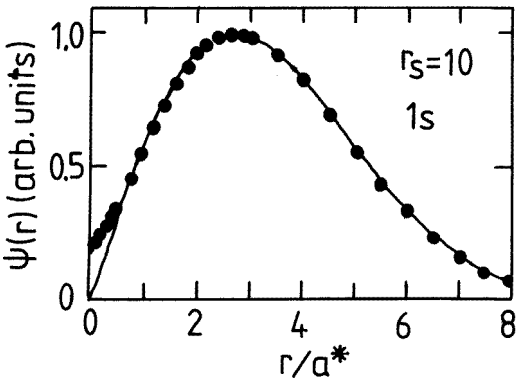

Figure 3. The wavefunction $\psi(r)$ of the ground state ($n_r = 1, l = 0$) for screened repulsive test charges for $r_s = 10$ versus r. The full circles show the results of the matrix diagonalization and the full curve represents the variational calculation.

3.2. The variational method

The screened potential near the minimum at $r_{\rm min}$ can be described by a one-dimensional oscillator potential. Therefore, we use as the variational wavefunction $\phi_{1v}(r) = Ar^{k_1/2}\exp(-r^2/2\alpha^2)$ with A as the normalization constant and given by $A^2 = 2/\Gamma[(k_1 + 2)/2]\alpha^{2+k_1}$. k_1 and α are the variational parameters. $\phi_{1v}(r)$ describes states with a given angular momentum l and $\phi_{1v}(r)$ has one node $n_r = 1$ at $r = 0$ if $k_1 > 0$. Solving the variational problem with this wavefunction gives bound states with quantum numbers $n_r = 1$

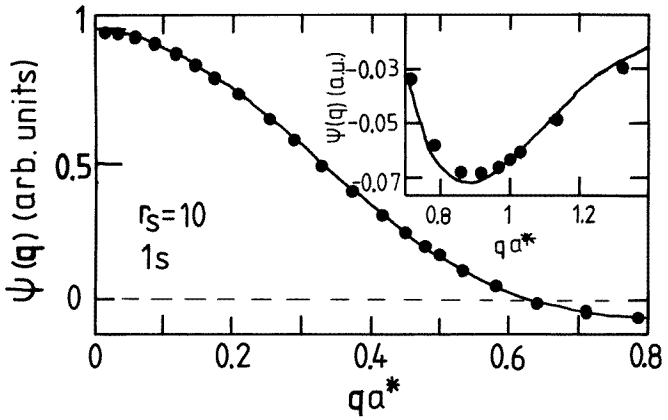

Figure 4. The wavefunction $\psi(q)$ of the ground state ($n_r = 1, l = 0$) for screened repulsive test charges for $r_s = 10$ versus wavenumber q. The full circles show the results of the matrix diagonalization and the full curve represents the variational calculation.

and $l = 0, 1, 2, \ldots$. The wavefunction $\phi_{1v}(r)$ shows a maximum at $r^* = (k_1/2)^{1/2}\alpha$.

We find for the radial wavefunction with $n_r = 1$ the analytical results $\langle T\rangle = \text{Rydberg}^* a^{*2}/\alpha^2$, $\langle V_l\rangle = 2\ \text{Rydberg}^* a^{*2} l^2/\alpha^2 k_1$ and

$$\langle V_{sc,t}\rangle = 2\ \text{Rydberg}^* a^* \int_0^\infty \mathrm{d}q\ {}_1F_1[1 + k_1/2;\ 1;\ -q^2\alpha^2/4]/\varepsilon(q) \tag{7}$$

where ${}_1F_1(x; y; z)$ is the degenerate hypergeometric function [21]. Some representative numerical results are given in table 1 for different r_s. The variational method provides energies only slightly higher than the exact results obtained by matrix diagonalization. The bound states are very extended in space due to the repulsive potential for $r \to 0$.

For the states with two nodes $n_r = 2$ we use for the radial wavefunction $\phi_{2v}(r) = B[r^{k_2/2} - Cr^{k_3/2}]\exp(-r^2/2\beta^2)$. $\phi_{2v}(r)$ describes the states with $n_r = 2$ and $l = 0, 1, 2\ldots$ and we find

$$\langle T\rangle = \text{Rydberg}^* \frac{a^{*2}}{2} B^2\beta^{k_2}\{\Gamma(k_2/2)k_2/2 + C^2\beta^{k_3-k_2}\Gamma(k_3/2)k_3/2 + C\beta^{k_3/2-k_2/2}\Gamma(k_2/4 + k_3/4)(k_2^2/8 + k_3^2/8 - k_2k_3/4 - k_2/2 - k_3/2)\} \tag{8a}$$

$$\langle V_l\rangle = \text{Rydberg}^* \frac{a^{*2}}{2} l^2 B^2\beta^{k_2}\{\Gamma(k_2/2) + C^2\beta^{k_3-k_2}\Gamma(k_3/2) - 2C\beta^{k_3/2-k_2/2}\Gamma(k_2/4 + k_3/4)\} \tag{8b}$$

and

$$\langle V_{sc,t}\rangle = \text{Rydberg}^* a^* B^2 \int_0^\infty \mathrm{d}q\ \frac{1}{\varepsilon(q)}\{\beta^{k_2+2}\Gamma(1 + k_2/2){}_1F_1[1 + k_2/2;\ 1;\ -q^2\beta^2/4] - 2C\beta^{k_2/2+k_3/2+2}\Gamma(1 + k_2/4 + k_3/4){}_1F_1[1 + k_2/4 + k_3/4;\ 1;\ -q^2\beta^2/4] + C^2\beta^{k_3+2}\Gamma(1 + k_3/2){}_1F_1[1 + k_3/2;\ 1;\ -q^2\beta^2/4]\}. \tag{8c}$$

With the normalization condition we derive

$$1/B^2 = \{\beta^{k_2+2}\Gamma(1 + k_2/2) - 2C\beta^{k_2/2+k_3/2+2}\Gamma(1 + k_2/4 + k_3/4) + C^2\beta^{k_3+2}\Gamma(1 + k_3/2)\}/2. \tag{9}$$

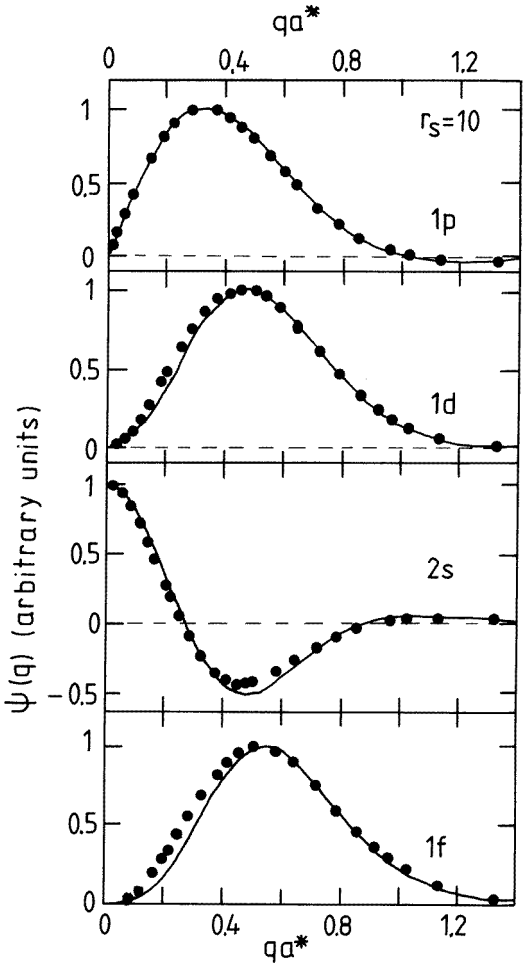

Figure 5. The wavefunction $\psi(q)$ of the first excited states ($n_r = 1, l = 1-3$ and $n_r = 2, l = 0$) for screened repulsive test charges for $r_s = 10$ versus wavenumber q. The full circles show the results of the matrix diagonalization and the full curve represents the variational method.

The condition for C follows from $\langle\phi_{1v}|\phi_{2v}\rangle = 0$ and we obtain

$$C = \left[\frac{2\alpha^2\beta^2}{\alpha^2+\beta^2}\right]^{k_2/4-k_3/4} \frac{\Gamma(1+k_1/4+k_2/4)}{\Gamma(1+k_1/4+k_3/4)}. \tag{10}$$

Numerical results of the bound-state energies found with the variational approach for the states $n_r = 2$ and $l = 0, 1, 2, \ldots$ are given in table 2 together with results from the matrix diagonalization.

Figure 2 represents a summary of the results concerning the binding energies as functions of r_s. Bound states are found for low and intermediate densities. They can either be calculated numerically by the matrix diagonalization method or by a quasi-analytical variational method. 3s and 3p states have been found by matrix diagonalization (see the dotted curves in figure 2).

Using the Bessel functions of the first kind the wavefunctions $\phi_l(r)$ can be Fourier transformed. One obtains

$$\phi_l(q) \propto \int_0^\infty \mathrm{d}r\, r J_l(qr)\phi_l(r). \tag{11}$$

Table 1. Bound-state energies $E_{\min}$ for a screened repulsive test charge found by the variational method together with the variational parameters α and k_1 for $\phi_{1v}(r)$ for different r_s values. The corresponding bound states E_{num} found by matrix diagonalization are also given.

r_s	State	l	α/a^*	k_1	$E_{\min}$/Rydberg*	E_{num}/Rydberg*
20	1s	0	3.645	2.493	−0.6482	−0.6496
20	1p	1	3.618	3.254	−0.5955	−0.5963
20	1d	2	3.677	4.612	−0.4811	−0.4816
20	1f	3	3.815	6.029	−0.3473	−0.3478
20	1g	4	4.008	7.385	−0.2109	−0.2117
20	1h	5	4.266	8.583	−0.0791	−0.0807
10	1s	0	2.818	1.832	−0.5563	−0.5589
10	1p	1	2.818	2.714	−0.4460	−0.4468
10	1d	2	2.978	4.019	−0.2343	−0.2362
10	1f	3	3.305	5.139	−0.0128	−0.0161
5	1s	0	2.299	1.272	−0.3403	−0.3428
5	1p	1	2.394	2.202	−0.1333	−0.1395
4	1s	0	2.204	1.100	−0.2432	−0.2542
3	1s	0	2.183	0.865	−0.1031	−0.1240
2.5	1s	0	2.358	0.668	−0.0139	−0.0496
2	1s	0	—	—	—	−0.0022 1

Table 2. Bound-state energies $E_{\min}$ for a screened repulsive test charge found by the variational method with $\phi_{2v}(r)$ together with the variational parameters β , k_2, and k_3 for different r_s values. The corresponding bound states E_{num} found by matrix diagonalization are also given.

r_s	State	l	β/a^*	k_2	k_3	$E_{\min}$/Rydberg*	E_{num}/Rydberg*
20	2s	0	3.826	2.201	6.408	−0.3490	−0.3522
20	2p	1	3.982	3.716	5.467	−0.3015	−0.3016
20	2d	2	4.093	5.808	5.808	−0.2044	−0.2051
20	2f	3	4.276	7.093	7.127	−0.0949	−0.0982
10	2s	0	3.281	1.828	4.607	−0.0795	−0.0851

For $l = 0$ the wavefunction in the momentum space is given by $\phi_l(q \to 0) =$ constant. For $n_r = 1$ and $n_r = 2$ the variational wavefunctions in the momentum space can be expressed in terms of degenerate hypergeometric functions [21]. We only give the explicit results for $n_r = 1$: equation (11) can be used directly in order to calculate $\phi_l(q)$. For $\phi_{1v}(r)$ we find

$$\phi_{1v}(q) \propto r^l {}_1F_1[1 + (k_1 + l)/2; 1 + l; -q^2\alpha^2/2). \tag{12}$$

Our result for the variational ground-state wavefunction for $r_s = 10$ is shown in figure 4 and agrees very well with the numerical result. For the $1p$, $1d$, $2s$ and $1f$ excited states the variational results for the wavefunction in the momentum space are shown in figure 5 and are in reasonable agreement with the corresponding results of the matrix diagonalization.

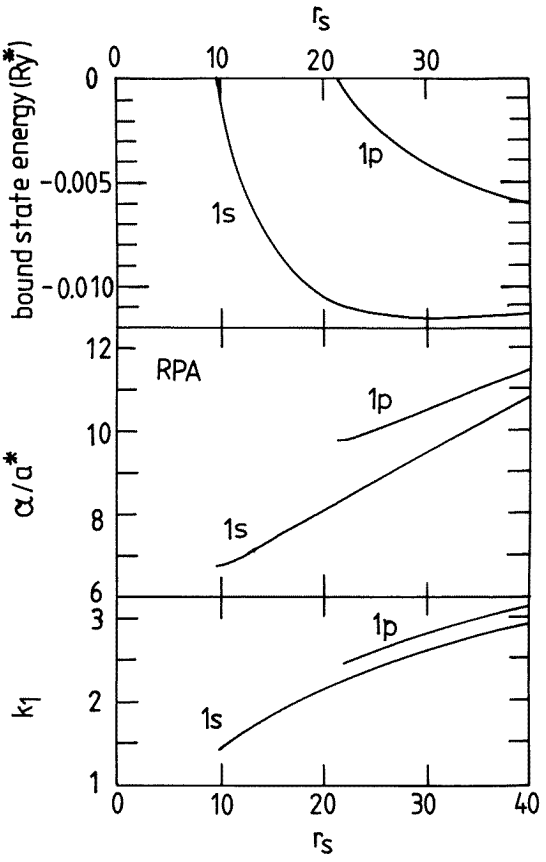

Figure 6. The bound-state energy E_{var} and variational parameters α and k_1 for screened repulsive test charges versus r_s are shown by the full curves for $n_r = 1$ and $l = 0$ (1s) and $l = 1$ (1p) within the RPA.

3.3. Different forms for the LFC

In this subsection we show that the existence of bound states in a screened repulsive potential is not a special property of the LFC given in equation (2). Even within the RPA, where $G(q) = 0$, we find bound states, however, the binding energy is small (see figure 6). Using $\phi_{1v}(r)$ we have studied the behaviour of the binding energy of the ground state and the first excited state versus r_s and found that bound states exist for $r_s > r_{sc\mathrm{RPA}} = 9.75$. Including the LFC we found bound states for $r_s > r_{sc} = 2.4$. We conclude that $r_{sc\mathrm{RPA}}/r_{sc} = 4.06$ which means that $N_c/N_{c\mathrm{RPA}} = 16.5$. Within the RPA the energy of the ground state is reduced by a factor of 56 compared with the calculation using the LFC.

The numerical values for the bound states depend on the form for the LFC. If we use the LFC as described in [10], where the LFC is parametrized by two coefficients, we obtain the results for the 1s state shown in figure 7. For $r_s > 3$ bound-state energies are found in good agreement with the results shown in figure 2. The critical density is somewhat lower than in figure 2. This shows that the existence of bound states is not a special property of our LFC formula. However, r_{sc} and the exact values of the binding energies for r_s near r_{sc} depend on the form chosen for the LFC.

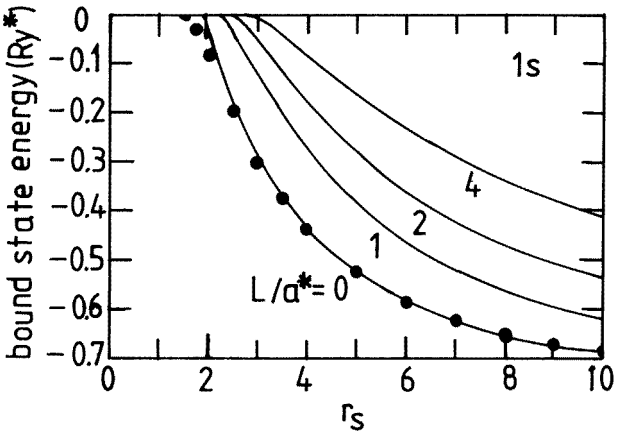

Figure 7. The bound-state energies for screened repulsive test charges in a quantum well versus r_s are shown by the full curves for $n_r = 1$ and $l = 0$ for different quantum well widths L. The full circles are calculated by matrix diagonalization for $L = 0$. The two-sum-rule approach [10] is used for the LFC.

3.4. Quantum wells with finite width

In order to study real two-dimensional systems we consider quantum wells with infinite barriers and a finite well width L in the z-direction. The interaction potential $V(q) = 2\pi e^2 F(qL)/\varepsilon_L q$ is modified by a form factor $F(x)$ [22]. The LFC for this model was discussed in [10] within the two-sum-rule approach where the coefficients $C_1(r_s, L)$ and $C_2(r_s, L)$ depend on the well width.

Our variational results for the 1s state are shown in figure 7 for different well widths. With increasing well width r_{sc} increases and the binding energy decreases. We have also studied excited states and the results are qualitatively similar to that shown in figure 2.

4. Screened attractive test charges

4.1. The attractive test-charge potential

In this section we study bound states between a positive and a negative test charge screened by the two-dimensional electron gas (attractive test-charge–test-charge interaction). The effects of screening within the RPA have already been considered in the literature [14–16]. To classify the states we use the notation of the hydrogen atom with n and l.

The screened potential for attractive test charges versus r is shown in figure 8. Already for $r_s = 4$ large differences are seen between the screened potential according to the RPA and when the LFC is taken into account. Many-body effects via the LFC lead to a weaker attractive potential.

4.2. Matrix diagonalization

Numerical results for the binding energy of the 1s state versus r_s are shown in figure 9 within the RPA and by including the LFC. With increasing density the binding energies decrease due to screening effects but unlike the three-dimensional case, where the ground-state energy

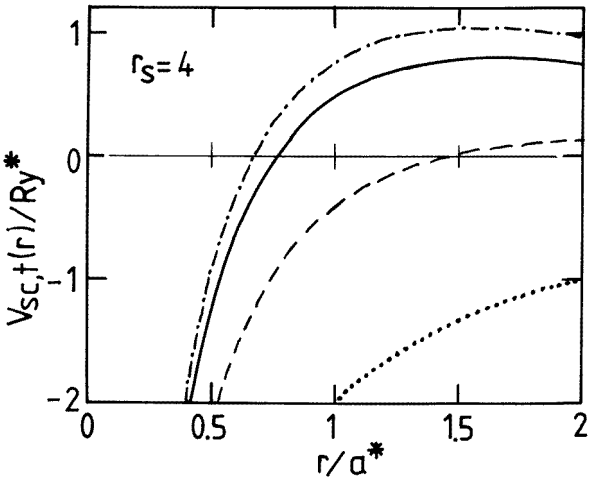

Figure 8. A screened Coulomb potential $V_{sc,t}(r)$ for attractive test charges versus distance r for $r_s = 4$ are shown by the full curves. The dotted curve represents the unscreened potential and the broken curve the RPA. To obtain the chain curve the LFC within the two-sum-rule approach [10] was used.

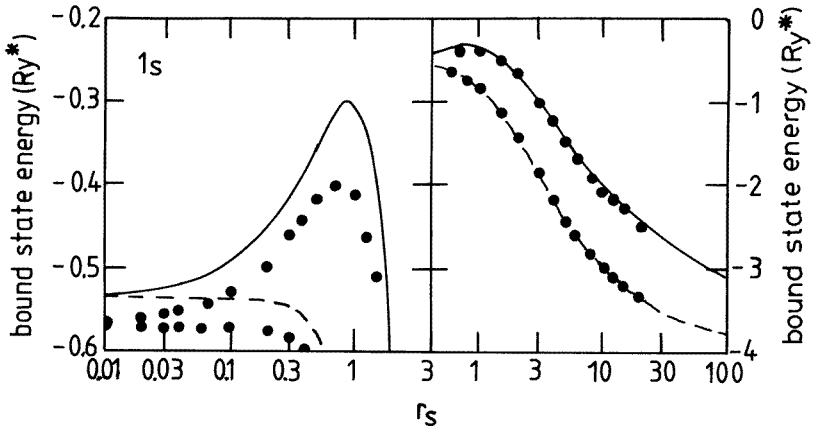

Figure 9. The ground-state energies for screened attractive test charges found by matrix diagonalization versus r_s are shown by the full circles. The variational results $E_{\min}$ are shown as full curves when the LFC is used and as broken curves for the RPA.

vanishes at Mott's critical density N_M [23], in two dimensions the binding energy remains finite even for $r_s \to 0$ [14]. Using the LFC gives rise to a smaller binding energy. The binding energy as a function of r_s has a minimum of -0.4 Rydberg* at $r_s = 0.8$. This minimum is induced by many-body effects and does not appear if the RPA is used for the screening function.

In the unscreened limit the binding energies are given by $E_n = -4$ Rydberg$^*/(2n+1)^2$ with $n = 0, 1, 2 \ldots$ [12]. The exact numerical result for the ground-state energy within the RPA as a function of r_s was given in [15]. Our results obtained by matrix diagonalization are in agreement with these results. This confirms the accuracy of our method: we find

-0.571 Rydberg*, -0.859 Rydberg* and -2.969 Rydberg* for $r_s = 0.01$, $r_s = 1$ and $r_s = 10$, respectively.

4.3. The variational method

In the variational method we use for the 1s ground state $\phi_{3v}(r) = A\exp(-r/2\nu)$ and we obtain $\langle T\rangle = \text{Rydberg}^* a^{*2}/4\nu^2$ and

$$\langle V_{sc,t}\rangle = \int_0^\infty \mathrm{d}q\, q\, V_{sc,t}(q)/[2\pi(1+q^2\nu^2)^{3/2}]. \tag{13}$$

Note that $V_l = 0$ for $l = 0$. Our results for the ground-state energy obtained with the variational method and using the RPA are shown in figure 9. The binding energies obtained with the variational method are somewhat smaller than the energies calculated by matrix diagonalization. For instance, for $r_s = 0.01$ we find -0.536 Rydberg* while the numerical eigenvalue is -0.571 Rydberg* which corresponds to a difference of 7%. Including the LFC in the variational method, the minimum of the binding energy is found at $r_s = 0.9$ with -0.298 Rydberg*, see figure 9. The Fourier transform of $\phi_{3v}(r)$ is given by $\phi_{3v}(q) \propto 1/(1+4q^2\nu^2)^{3/2}$. We have checked that $\phi_{3v}(q)$ versus q for $r_s = 4$ is in very good agreement with the result obtained by matrix diagonalization.

For the first excited state (2s state) we use $\phi_{4v}(r) = A(1-rD)\exp(-r/2\kappa)$. The different terms of the variational energy are given by

$$\langle T\rangle = \text{Rydberg}^* \frac{a^{*2}}{4\kappa^2}\frac{1+2\nu/\kappa+9\nu^2/\kappa^2}{3-2\nu/\kappa+3\nu^2/\kappa^2} \tag{14a}$$

and

$$\langle V_{sc,t}\rangle = \frac{1}{2\pi}\int_0^\infty \mathrm{d}q\, q\, V_{sc,t}(q)\frac{1}{(1+q^2\kappa^2)^{7/2}} \times\left\{1+\frac{q^2\kappa^2[15-26\kappa/\nu-9\kappa^2/\nu^2]+q^4\kappa^4[24+8\kappa/\nu]}{6-4\kappa/\nu+6\kappa^2/\nu^2}\right\} \tag{14b}$$

with $V_l = 0$ for $l = 0$. The orthogonalization $\langle\phi_{3v}|\phi_{4v}\rangle = 0$ implies that $D = (1/\nu+1/\kappa)/4$. For the second excited state (2p state) we use $\phi_{5v}(r) = Ar\exp(-r/2\mu)$ and we obtain $\langle T\rangle = \text{Rydberg}^* a^{*2}/12\mu^2$, $\langle V_l\rangle = \text{Rydberg}^* a^{*2}l^2/6\mu^2(l=1)$ and

$$\langle V_{sc,t}\rangle = \frac{1}{2\pi}\int_0^\infty \mathrm{d}q\, q\, V_{sc,t}(q)\frac{1-3q^2\mu^2/2}{(1+q^2\mu^2)^{7/2}}. \tag{15}$$

Results for the 2s and 2p states and using the RPA are shown in figure 10. These states only exist for $r_s > 27$ and the 2s state is slightly lower in energy than the 2p state. These states are well described by hydrogenic wavefunctions. When screening effects via the RPA are included the 2s state and the 2p states are no longer degenerate, but the splitting between 2s and 2p is small. Excited states in two-dimensional systems have only been studied for unscreened impurities in quantum wells [24].

4.4. Bound states induced by Friedel oscillations

Inclusion of the LFC in the screening function dramatically changes the results for the excited states: we find excited states already for $r_s > 4$. Within the RPA excited bound states only exist for $r_s > 27$. Many-body effects enhance Friedel oscillations [4]. The binding energies and the number of excited states are determined by the attractive part of the first (Friedel) minimum in the screened potential. In fact, when the LFC is included, it is possible

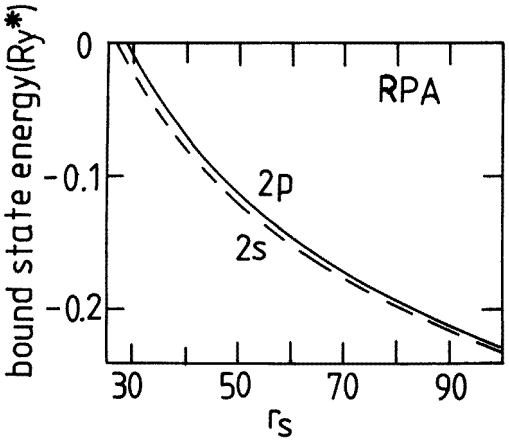

Figure 10. The excited-state energies for screened attractive test charges found by the variational method versus r_s.

Table 3. Bound states between screened attractive test charges found by matrix diagonalization and with the variational approach including the LFC for $r_s = 10$. The values in curly brackets represent variational parameters. At r_m the variational wavefunction has a maximum.

r_s	l	nl	$E_{\rm num}$/Rydberg*	$E_{\rm min}$/Rydberg*	r_m/a^*
10	0	1s	-2.083	-1.963 $\{\nu = 0.252a^*\}$	0.0
(10	0	1s	-2.083	-1.101 $\{k_1 = 0, \alpha/a^* = 0.57\}$	0.0)
10	0	2s	-0.059	-0.0590 $\{k_2 = 11.63, k_3 = 5.54, \beta/a^* = 5.62\}$	13.5
10	1	1p	-0.055	-0.0537 $\{k_1 = 11.75, \alpha/a^* = 5.64\}$	13.7
10	2	1d	-0.039	-0.0380 $\{k_1 = 12.00, \alpha/a^* = 5.70\}$	13.9
10	3	1e	-0.015	-0.0131 $\{k_1 = 12.28, \alpha/a^* = 5.83\}$	14.4

to use the same notation for the excited states as for the repulsive test-charge–test-charge interaction. This is supported by the good agreement between the matrix diagonalization method and the variational approach for the excited states using Gaussian wavefunctions for the excited states. The important point is that the variational wavefunction $\phi_{1v}(r)$ exhibits a maximum at $r_m = r^*$ which fits with the minimum $V_{sc,t}(r_F)$ of the first Friedel oscillation at r_F. In contrast, for the 1s ground state, the binding energy is determined by the large attractive part of the potential near $r = 0$.

The binding energies for excited states obtained by matrix diagonalization versus r_s are shown in figure 11. For large r_s the first (Friedel) minimum is located at a large distance (where $V_l(r)$ is small) and states with different l are not very different in energy. This is the reason why for $r_s > 15$ the number of excited states increases dramatically. For large r_s the order of magnitude of the binding energy is -0.05 Rydberg*: the energy scale of the first (Friedel) minimum (see the inset in figure 11), is -0.1 Rydberg*. The energy values obtained by both methods are in reasonable agreement, see table 3 and figure 11. When r_s increases r_F also increases while $V_{sc,t}(r_F)$ remains nearly constant (see the inset in figure 11). The reduction of the binding energy of the excited states with decreasing r_s is due to the increasing positive part of $V_l(r)$ with decreasing r_F.

In table 3 we compare for $r_s = 10$ the results for the binding energy obtained by matrix

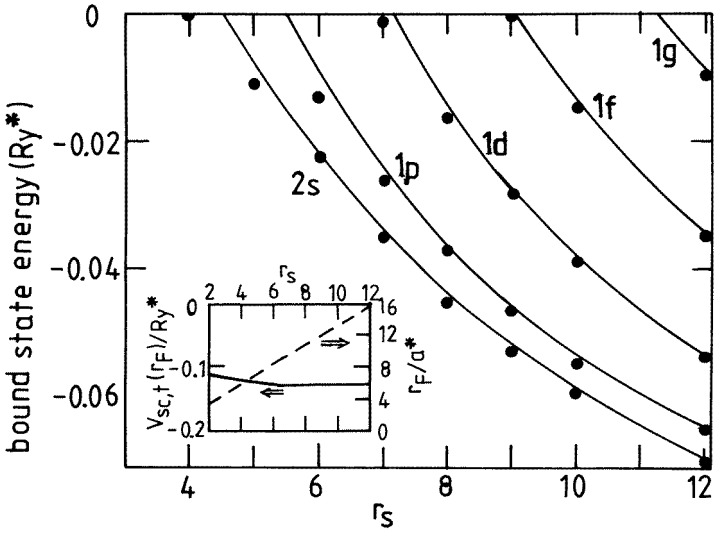

Figure 11. The excited-state energies for screened attractive test-charges found by matrix diagonalization versus r_s are shown by the full circles. The LFC is included. The full curves represent the variational calculation. In the inset the r_s dependence of the first (Friedel) minimum of the screened potential, characterized by r_F and $V_{sc,t}(r_F)$, is shown.

diagonalization with the results of the variational approach. The first (Friedel) minimum with $r_F = 13.2a^*$ and $V_{sc,t}(r_F) = -0.131$ Rydberg* for $r_s = 10$ controls the binding energy: the states 1p, 1d, and 1f are characterized by similar values of r_m, where the wavefunction shows a maximum. In figure 12 we show in the Fourier space the wavefunctions obtained numerically. We checked that these results can be well described by the Fourier transform of $\phi_{1v}(r)$ for the 1p, 1d, and 1f states and by $\phi_{2v}(r)$ for the 2s state. The 1s state is described by $\phi_{3v}(r)$.

Using the LFC, we have also applied the variational method with an exponential behaviour for the excited states. The binding energies obtained are roughly one order of magnitude smaller than the binding energies found with the Gaussian form. This supports our argument that the LFC leads to a qualitative change of excited bound states.

5. Discussion

We have discussed the screened potential between two *test charges* which are distinguishable from the electrons providing the screening. The motivation for using test charges is that the screened potential is known if the LFC for charge-density fluctuations is known. However, we recently analysed the test-charge–electron interaction [25] where a different form for the screening function [26] takes account of the indistinguishability (exchange) of the bound electron and the electrons responsible for the screening. It was found that the binding energies are much smaller than in the case of the test-charge–test-charge interaction.

In [4] we have studied, within the Kukkonen and Overhauser approach [26], the electron–electron interaction by using only exchange effects in the LFC. Spin effects and the indistinguishability of the electrons were taken into account. We concluded that the screened test-charge–test-charge interaction potential gives a good estimate of the effective electron–electron interaction potential [4]. For a study of the effective electron–electron

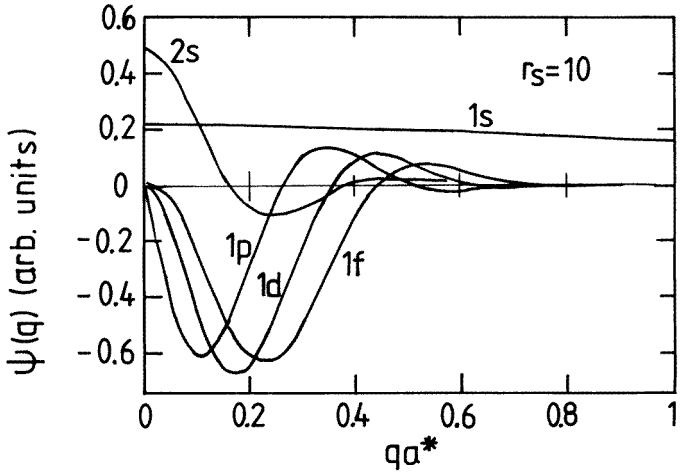

Figure 12. The wavefunction $\psi(q)$ of the ground state (1s) and the first excited states ($n_r = 1, l = 1$–3 and $n_r = 2, l = 0$) for screened attractive test charges for $r_s = 10$ versus the wavenumber q as obtained by matrix diagonalization. The LFC is included.

interaction and spin effects the LFC for spin-density fluctuations has to be calculated and this will be reported elsewhere.

For the three-dimensional electron gas an approach similar to the Kukkonen and Overhauser approach was recently used to calculate the critical temperature for superconductivity in systems with electron–phonon interaction and electron–electron interaction [27]. Good agreement with experiments was reported. We have also studied the three-dimensional electron gas [28]. For repulsive test-charges the 1s state binding energy saturates at -0.065 Rydberg* at low densities. We conclude that the binding energies in three-dimensional systems are smaller than in two dimensions, where we obtain a saturation at -0.65 Rydberg*.

6. Conclusion

We have studied bound states between two negative (repulsive) test charges and between a positive and a negative (attractive) test charge screened by a two-dimensional electron gas of given density. For repulsive test charges we found bound states at low electron densities $r_s > r_{sc} \approx 2$–3. The binding energy of the ground state saturates at low density at about -0.65 Rydberg*. For *attractive* test charges we found bound states for all densities. The binding energies of excited states are increased due to Friedel oscillations enhanced by many-body effects. We predicted excited states bound by the attractive part of the first Friedel oscillation.

References

[1] Pines D and Nozières P 1966 *The Theory of Quantum Liquids* vol 1 (New York: Benjamin)
[2] Kohn W and Luttinger J M 1965 *Phys. Rev. Lett.* **15** 525
[3] Wigner E 1934 *Phys. Rev.* **46** 1002
[4] Gold A 1994 *Phil. Mag. Lett.* **70** 141
[5] Calmels L and Gold A 1995 *Phys. Rev.* B **51** 8426

[6] Ghazali A and Gold A 1995 *Phys. Rev.* B **52** 16 634
[7] Singwi K S, Tosi M P, Land R H and Sjölander A 1968 *Phys. Rev.* **176** 589
[8] Jonson M 1976 *J. Phys. C: Solid State Phys.* **9** 3055
[9] Singwi K S and Tosi M P 1981 *Solid State Physics* vol 36 (New York: Academic) p 177
[10] Gold A and Calmels L 1993 *Phys. Rev.* B **48** 11 622
[11] Gold A 1997 *Z. Phys.* B **103** 491
[12] Flügge S 1965 *Rechenmethoden der Quantentheorie* 3rd edn (Berlin: Springer)
[13] Bastard G 1980 *Phys. Rev.* B **24** 4714
[14] Hipólito O and Campos V P 1979 *Phys. Rev.* B **19** 3083
Brum J A, Bastard G and Guillemot C 1984 *Phys. Rev.* B **30** 905
[15] Ackleh E S, Mahan G D and Wu J-W 1994 *Mod. Phys. Lett.* **8** 1041
[16] Stern F 1973 *Phys. Rev. Lett.* **30** 278
[17] Tanatar B and Ceperley D M 1989 *Phys. Rev.* B **39** 5005
[18] Shaw R W Jr 1970 *J. Phys. C: Solid State Phys.* **3** 1140
Kimball J C 1973 *Phys. Rev.* A **7** 1648
[19] Nagano S, Singwi K S and Ohnishi S 1984 *Phys. Rev.* B **29** 1209
Nagano S, Singwi K S and Ohnishi S 1985 *Phys. Rev.* B **31** 3166 (erratum)
[20] Moroni S, Ceperley D M and Senatore G 1990 *Phys. Rev. Lett.* **64** 303
[21] Gradshteyn I S and Ryzhik I M 1980 *Table of Integrals, Series, and Products* (New York: Academic)
[22] Gold A 1987 *Phys. Rev.* B **35** 723
[23] Mott N F 1949 *Proc. Phys. Soc.* **162** 416
[24] Greene R L and Bajaj K K 1983 *Solid State Commun.* **45** 825
[25] Gold A and Ghazali A 1997 *J. Phys.: Condens. Matter* **9** 3749
[26] Kukkonen C A and Overhauser A W 1979 *Phys. Rev.* B **20** 550
[27] Richardson C F and Ashcroft N W 1996 *Phys. Rev.* B **54** R764
[28] Gold A and Ghazali A 1996 *J. Phys.: Condens. Matter* **8** 7393